Global dryland aridity changes indicated by atmospheric, hydrological, and vegetation observations at meteorological stations

Haiyang Shi[1,~~6~~8], Geping Luo[2,3,4,6], Olaf Hellwich[7], Xiufeng ~~He[1]~~He[8], Alishir Kurban[2,3,4,6], Philippe De Maeyer[2,3,5,6] and Tim Van de Voorde[5,6]

[1] ~~School~~Department of ~~Earth Sciences~~Civil and Environmental Engineering, ~~Hohai~~ University~~, Nanjing 211100, China~~ of Illinois at Urbana-Champaign, Urbana, IL 61801, USA.
[2] State Key Laboratory of Desert and Oasis Ecology, Xinjiang Institute of Ecology and Geography, Chinese Academy of Sciences, Urumqi, Xinjiang, 830011, China.
[3] College of Resources and Environment, University of the Chinese Academy of Sciences, 19 (A) Yuquan Road, Beijing, 100049, China.
[4] The National Key Laboratory of Ecological Security and Sustainable Development in Arid Region ~~(proposed),~~, Chinese Academy of Sciences, Urumqi, China.
[5] Department of Geography, Ghent University, Ghent 9000, Belgium.
[6] Sino-Belgian Joint Laboratory of Geo-Information, Ghent, Belgium.
[7] Department of Computer Vision & Remote Sensing, Technische Universität Berlin, 10587 Berlin, Germany.

[8] School of Earth Sciences and Engineering, Hohai University, Nanjing 211100, China.

Correspondence to: Geping Luo (luogp@ms.xjb.ac.cn) and Olaf Hellwich (olaf.hellwich@tu-berlin.de)

Submitted to: *Hydrology and Earth System Sciences*

Abstract

In the context of global warming, an increase in atmospheric aridity and global dryland expansion were expected under the future climate in previous studies. However, it conflicts with observed greening over drylands and the insignificant increase in hydrological and ecological aridity from the ecohydrology perspective. Combining climatic, hydrological, and vegetation data, this study evaluated global dryland aridity changes at meteorological ~~sites~~stations from 2003 to 2019. A decoupling between atmospheric, hydrological, and vegetation aridity was found. Atmospheric aridity represented by the vapour pressure deficit (VPD) increased, hydrological aridity indicated by machine learning-based precipitation minus evapotranspiration (P-ET) data did not change significantly, and ecological aridity represented by leaf area index (LAI) decreased. P-ET showed non-significant changes in most of the dominant combinations of VPD, LAI, and P-ET. This study highlights the added values of using station scale data to assess dryland change as a complement to the results based on coarse resolution reanalysis data and land surface models.

1 Introduction

Drylands are defined as regions with a dry climate, limited water, and scarce vegetation (Berg and McColl, 2021). In the context of global warming, the global dryland is expected to expand due to potential higher atmospheric water demand~~, the global dryland is expected to expand~~. It will severely affect the relevant ecosystem functions and livelihoods in drylands (Reynolds et al., 2007; Yao et al., 2020; Prăvălie, 2016). To date, there are still major limitations in the consensual knowledge and consistent understanding of global dryland aridity changes, such as wet-dry changes, the location, magnitude, and persistence of the potential dryland expansion and associated mechanisms (Berg and McColl, 2021; Lian et al., 2021; Huang et al., 2016, 2017; Grünzweig et al., 2022; Pan et al., 2021). Such knowledge gaps have substantially limited the effective climate adaptation and related strategy development to realize the Sustainable Development Goals in drylands, especially in the global south (Li et al., 2021; Fu et al., 2021; Yao et al., 2021; Ramón Vallejo et al., 2012).

The difficulty of the current investigation on dryland change lies in its multifaceted nature including the diverse characteristics of climate, hydrology, and ecosystems. The indicators and methods used to assess changes in drylands are thus diverse and previous studies have obtained different findings (Lian et al., 2021) on dryland change. ~~Typically, the arid index (AI),~~Typically, the arid index (AI) (Programme, 1997), calculated as the multi-year average precipitation (P) divided by potential evaporation (PET), was commonly used to measure atmospheric aridity in long-term global dryland change measuring studies (Huang et al., 2017, 2016). It used only atmospheric inputs, focused only on atmospheric aridity, and did not take into account the effects of ecohydrological aridity and the influence of land surface processes (Berg and McColl, 2021). AI-based studies have found global dryland expansions in the past and future (Huang et al., 2017, 2016) in the global warming context. However, such AI-based finding appears to be contrary to the global greening of dryland vegetation based on satellite remote sensing observations (Fensholt et al., 2012; Poulter et al., 2014; Lian et al., 2021; Hickler et al., 2005; Zhu et al., 2016). This illustrated the necessity of incorporating changes in surface properties such as vegetation in addition to atmospheric indicators. Therefore, from an ecohydrological perspective, recent studies have employed various ecohydrological indicators and land-surface-property changes such as soil moisture, vegetation greenness, evapotranspiration (ET), P-ET (i.e., P minus ET as surface water availability), and runoff to assess the dryland change (Berg and McColl, 2021; Lian et al., 2021; Denissen et al., 2022; Yang et al., 2018; Milly and Dunne, 2016; He et al., 2019). Such recent studies have shown that the dryland changes indicated by land surface changes and ecohydrological indicators did not confirm the 'expansion of drylands' finding in previous atmospheric-indicator-based studies (Huang et al., 2016, 2017; Feng and Fu, 2013). In terms of the mechanism explanation, these studies claimed that atmospheric drying and vegetation greening may occur simultaneously, and elevated vapour pressure deficit (VPD) does not fully propagate to surface changes to exacerbate decreases in soil moisture and runoff. Under elevated atmospheric CO_2, plant stomata may close and reduce transpiration and ET, and improve water use efficiency (WUE) (Lian et al., 2021; Berg and McColl, 2021; Roderick et al., 2015), which may compensate for the negative effects of elevated VPD on vegetation growth. This mechanism was not accounted for the physically based estimates of PET (e.g., the Penman-Monteith equation) and thus AI-based findings may have overestimated the aridity and contained considerable uncertainty.

However, the data used in most of the above-mentioned approaches have large uncertainties, such as coarse transpiration/ soil moisture data (0.5° × 0.5° resolution) from long-term climate and land surface model simulations (Berg and McColl, 2021) and coarse soil moisture/ ET data (0.25° × 0.25° resolution) from the Global Land Evaporation Amsterdam Model (GLEAM) or the global land data assimilation system (GLDAS), which are not necessarily applicable to the assessment of dryland expansion at fine scales. In addition, it is difficult to validate the findings in such coarse-resolution studies with ground observations. It is thus essential to make better use of station-scale data, which may have the potential in measuring dryland change at a finer scale, be better combined with ground observations, and provide more effective climate change adaptation suggestions for local communities.

Therefore, aimed at reducing scale-related uncertainty and obtaining a comprehensive finding of multifaceted characteristics, this study investigated dryland change at the meteorological station scale using the combinations of atmospheric, hydrological, and vegetation condition observations including VPD, P-ET, and leaf area index (LAI). VPD and P are from meteorological observations, LAI is from MODIS imagery. ET is estimated by a Random Forest (RF) model trained from dryland flux stations in FLUXNET2015, and the data-driven methods can avoid uncertainties caused by physically based ET models. At the station scale, this study provides new insights into global dryland aridity change using multifaceted data with a higher proportion of observations.

2 Methodology

We produced ET data for global dryland meteorological stations by applying an ET machine learning model obtained from FLUXNET2015's dryland flux station (AI < 0.65) data trained using RF to global dryland (AI < 0.65) meteorological stations. We selected daily ET observations (i.e., latent heat observations) from the FLUXNET2015 dataset for stations in drylands as the target variable. The selected predictor variables include downward shortwave radiation (RSDN), air temperature (Ta), daily variance (half-hourly daily maximum temperature minus daily minimum temperature, TArange), VPD, wind speed (WS), and LAI from remote sensing (Table 1).

The RF model was constructed using the RandomForestRegressor function from the scikit-learn package of Python. The parameter ‘n_estimators’ was set to 500, and default parameter values were used for the other parameters (Zhao et al., 2019). For the evaluation of model performance, we used a leave-one-station-out cross-validation approach used in previous studies of ET predictions (Tramontana et al., 2016; Zhang et al., 2021; Shi et al., 2022). It is a type of cross-validation approach in which each station’s observation is considered as the validation set and the rest stations’ observations are considered as the training set. It can help us understand the potential adaptability of the model to new data in the prediction set. Feature importance (IMP) was used to measure the contributions of predictors, and we adopted the permutation importance indices to represent IMP due to their reliability (Díaz-Uriarte and Alvarez de Andrés, 2006; Strobl et al., 2008; Grömping, 2009; Zhang et al., 2021) in RF models.

Finally, the ~~parameter-optimized~~constructed RF model was applied to the stations in the drylands of the global meteorological stations in the Global Surface Summary of the Day (GSOD) dataset. In this way, daily-scale ET time series data were predicted for each meteorological station. For each station, when the number of predicted daily ET records for a given year exceeded 100, the annual ET mean was calculated using the arithmetic mean of the daily ET values. Given the absence of data such as LAI during winter snowpack at a small number of arid zone stations, this approach allows for an effective dense sampling of growing season days to represent annual ET and distinguish between high and low annual ET values across years. In the subsequent formal dryland change analysis, cropland meteorological stations were removed due to potential considerable irrigation influence.

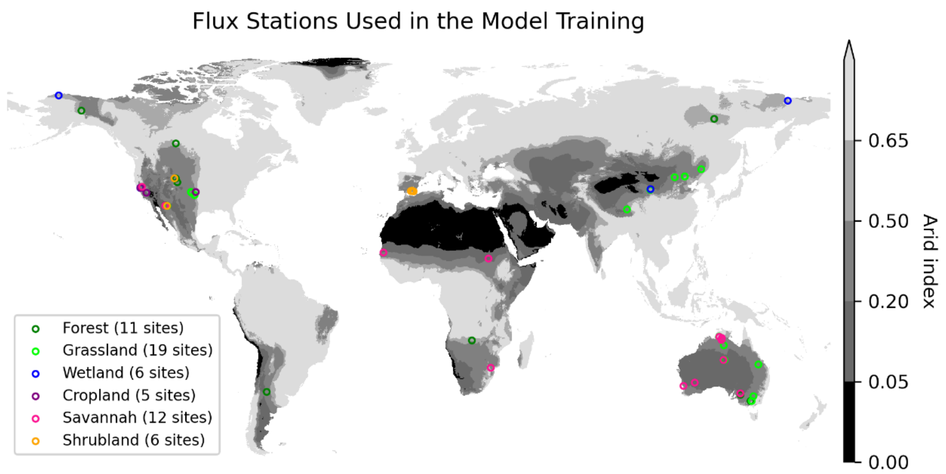

Figure 1 The used 59 flux ~~sites~~stations in drylands (AI < 0.65) in FLUXNET2015 in the RF model construction. AI level classification~~:~~ (Programme, 1997): hyperarid (0 < AI < 0.05), arid (0.05 < AI < 0.2), semiarid (0.2 < AI < 0.5), dry subhumid (0.5 < AI < 0.65).

Table 1. Description of the predictors used in the RF model to estimate ET at meteorological stations.

Predictor	Source	Description
LAI	MCD15A3H dataset derived from MODIS data	The 4-daily LAI was linearly interpolated to the daily scale. It was extracted based on Google Earth Engine (GEE) at a scale of 500 m (i.e., cutouts of the 500 × 500 m pixels centered on each station).
RSDN	from the BESS(Ryu et al., 2018) dataset derived from MODIS imagery	It is of 5.5 km spatial resolution. It was extracted based on GEE at a scale of 500 m
WS	In-situ observation	
TA	In-situ observation	
TArange	In-situ observation	Daily TArange is derived from the half-hourly maximum temperature and minimum temperature data of FLUXNET2015.

VPD	In-situ observation	VPD is calculated from TAmax, TAmin, and dew point temperature (Tdew) (Howell and Dusek, 1995).

3 Results

3.1 ET estimation evaluation

We evaluated the performance of the RF model at each flux ~~site~~station using leave-one-~~site~~station-out cross-validation, and most ~~sites~~stations showed high accuracy (Fig. 2) in both ~~Pearson's~~Pearson’s correlation coefficients (Rcorr) of observed and predicted daily ET values and the root mean square error (RMSE~~.~~). It indicated the feasibility of accurate daily ET simulations at most dryland flux ~~sites~~stations. And among the predictors, LAI had the highest ~~feature importance~~IMP (Fig. 2d), followed by RSDN, TA, WS, VPD, and TARange. This demonstrated the importance of surface vegetation conditions in ET simulations at dryland ~~sites~~stations.

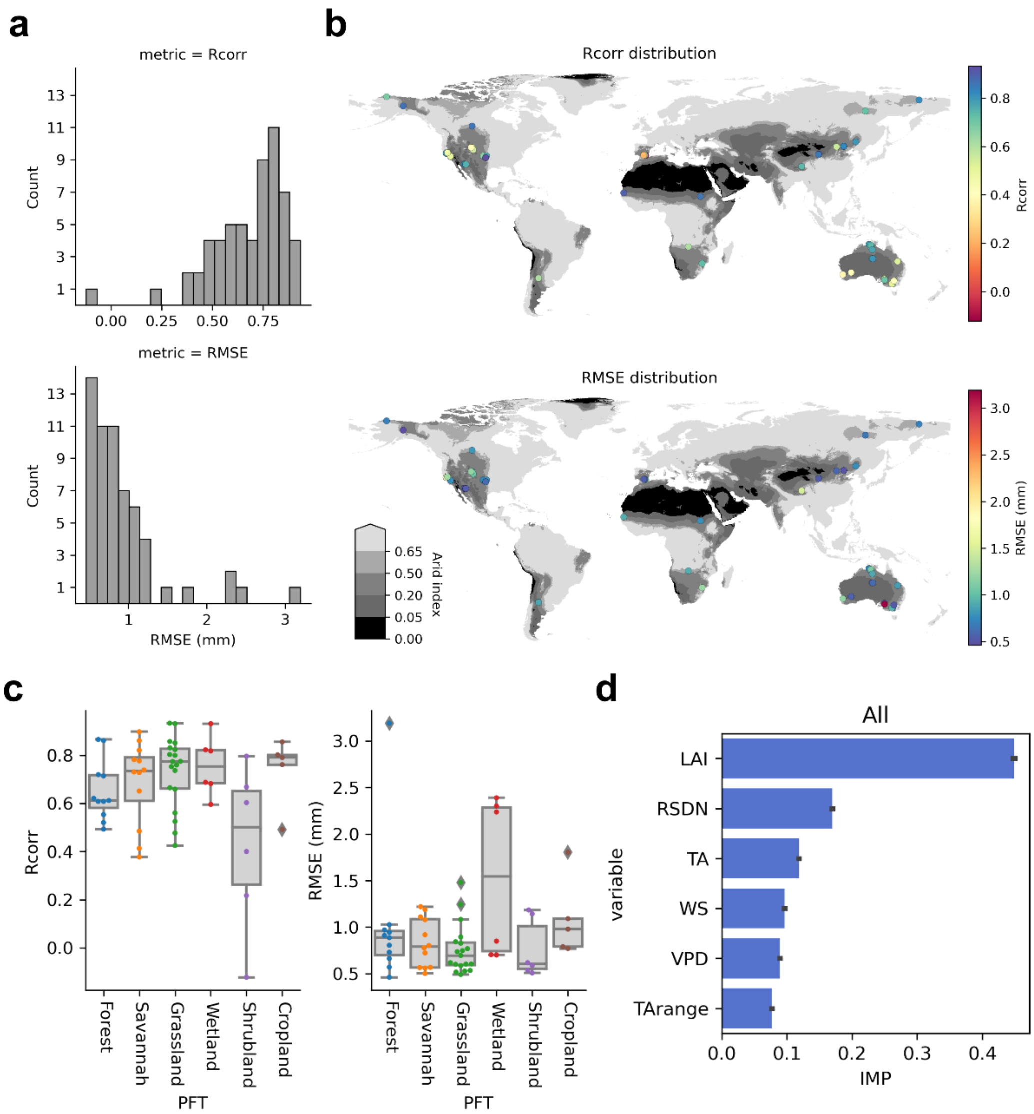

Figure 2 The model performance and feature importance in the leave-one-~~site~~station-out cross-validation. (a) Rcorr and RMSE values of 59 ~~sites~~stations. (b) Spatial distribution of Rcorr and RMSE records. (c) Rcorr and RMSE of various PFTs. (d) Feature importance (IMP) ranking.

3.2 Climatic, hydrological, and vegetation changes over drylands

The pattern of change in each climate and vegetation variable between the periods 2003-2010 and 2011-2019 showed considerable variations (Fig. 3). The number of ~~sites~~stations with significant increases in TA, LAI, and VPD was considerably greater than the number of ~~sites~~stations with significant decreases. The number of ~~sites~~stations with significant increases in P, ET, and P-ET was also greater than the number of ~~sites~~stations with significant decreases. The ratio of the numbers of ~~sites~~stations with increases and decreases in P-ET is the lowest. This shows the spatial variability of the trends indicated by the different indicators: the increase in TA and VPD in the context of global warming is widespread and their spatial pattern similarity is also high. The increasing trend in LAI is also dominant. The spatial pattern of ET changes is highly similar to that of LAI. Both ET and LAI show significant regional increases in the high latitudes of North America, and central Eurasia, and decreases in the middle and low latitudes of North America. The spatial pattern of changes in P-ET is more similar to that of P, but the increase in P is not completely propagated to P-ET and may be partially offset by the trend in ET.

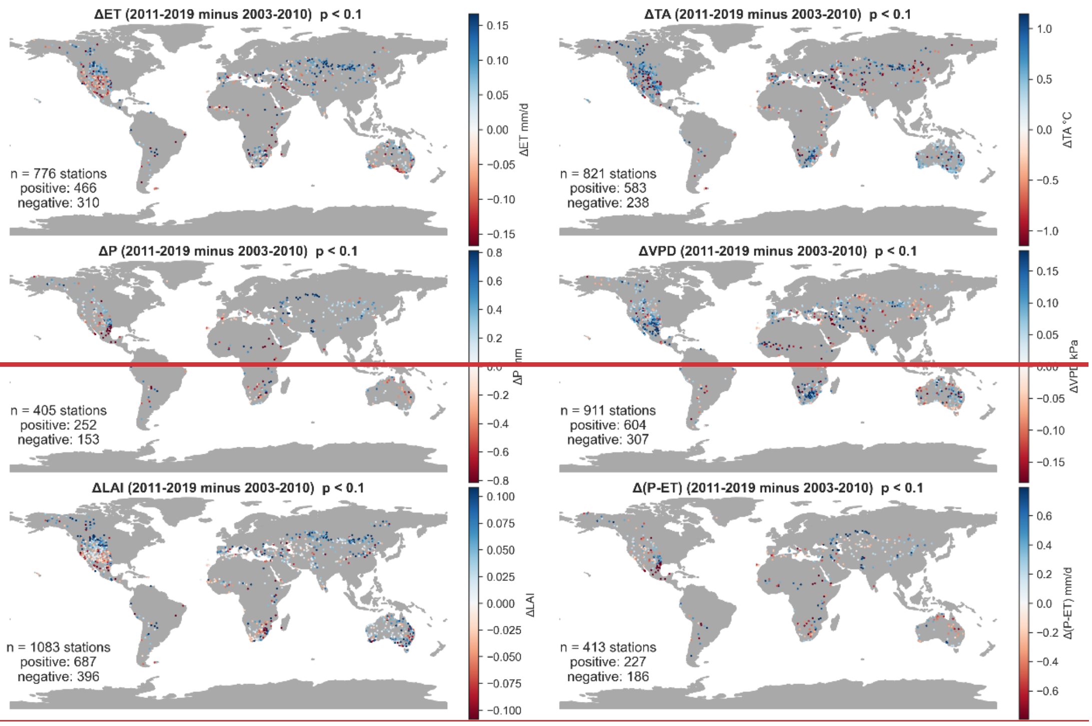

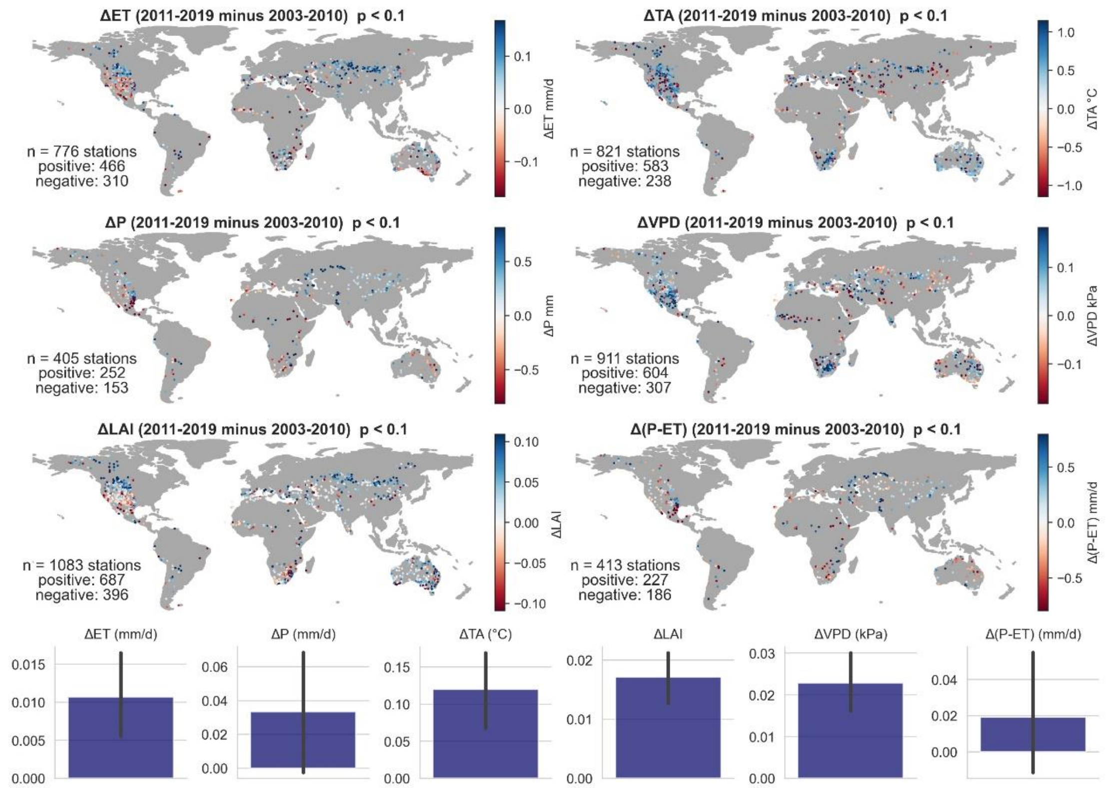

Figure 3 Significant changes ($p < 0.1$) in ET, TA, P, VPD, LAI, and P-ET for dryland meteorological ~~sites~~stations (from 2003-2010 to 2011-2019).

We compared the relationship between ΔVPD, which represents changes in atmospheric aridity, ΔP-ET, which represents changes in hydrological aridity, and ΔLAI, which represents changes in vegetation growth. ΔVPD showed a negative correlation with ΔP-ET ($R = -0.19$, $p < 0.001$), indicating that elevated VPD in drylands did lead to a decrease in surface water availability. However, the negative correlation between ΔVPD and ΔLAI was not strong ($R = -0.13$, $p < 0.001$), indicating that atmospheric drying was not a dominant determinant of vegetation greening or browning. The positive correlation between ΔP-ET and ΔLAI was not significant ($p > 0.1$), indicating a decoupling between the greening of dryland vegetation and changes in surface water availability.

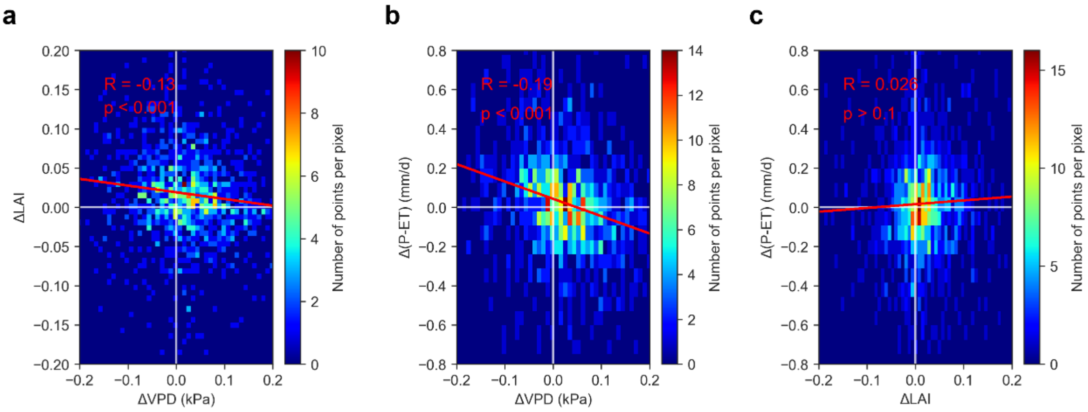

Figure 4 Relations of (a) ΔLAI-ΔVPD, (b) Δ(P-ET)-ΔVPD, and (c) Δ(P-ET)-ΔLAI at dryland meteorological ~~sites~~stations (from 2003-2010 to 2011-2019).

3.3 Combined atmospheric, hydrological, and vegetation perspectives

We also analyzed the combinations of VPD, LAI, and P-ET changes, and the distribution patterns of the different combinations across the globe represented different mechanisms of dryland changes (Fig. 5). In the Dry subhumid, Semiarid and Arid regions, three of the top four combinations exhibited significant increases in LAI, while VPD exhibited increases, no significant change, increases, and decreases, respectively. In the top four combinations, the combination with an increase in VPD accompanied by LAI decrease only ranked third or fourth. This suggests that the effect of vegetation browning caused by increasing VPD may not be dominant and that the increasing atmospheric water demand did not considerably decrease vegetation growth. In the Dry subhumid region, compared to the Semiarid and Arid regions, the combinations of 'VPD↓ & LAI↑ & P-ET (-)' and 'VPD↓ & LAI↑ & P-ET↑ ' combinations ranked higher. It indicates that in the Dry subhumid region, the possibility of the combination of VPD decrease accompanied by LAI increase is higher. In the Arid region, the combination of 'VPD↑ & LAI↑ & P-ET (-)' dropped from the first to the second in the ranking compared to the Dry sub-humid and Semiarid regions, indicating that when AI is lower, the mechanism represented by the combination of the simultaneous increase in VPD and LAI are less likely to occur. Surprisingly, of the seven combinations of VPD, LAI, and P-ET in the top ranking, P-ET showed no significant change. This suggests a smaller contribution from changes in surface water availability in explaining the variation of combinations of mechanisms for dryland change, although the changes in P-

ET and VPD in the lower-ranked combinations showed ~~opposite~~oppostation trends. The surface water represented aridity increase obtained in this study is smaller than that indicated by soil moisture and runoff reported previously (Lian et al., 2021).

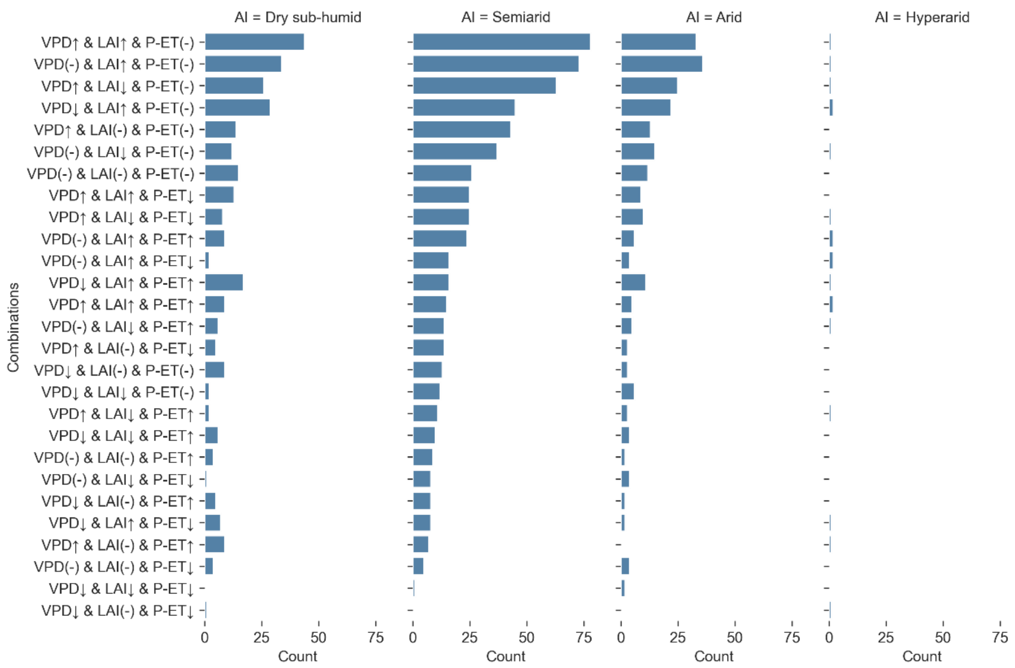

Figure 5 Combinations of VPD, LAI, and P-ET changes across various AI areas from 2003-2010 to 2011-2019. The symbol '↑' represents a significant increase ($p < 0.1$) of VPD, LAI, or P-ET. The symbol '↓' represents a significant decrease ($p < 0.1$) and '(-)' represents insignificant changes.

The distribution of these combinations is also highly heterogeneous spatially, indicating the high regional heterogeneity in global dryland change (Feng et al., 2022; Lian et al., 2021). Given this study is at the station scale, the impacts of heterogeneous underlying surface conditions can be higher. Combinations with non-significant changes in P-ET are widely distributed globally (Fig. 6a,b,c,d,e,f,g), including in the western part of North America, Australia, and southern Europe, where there are more dense stations. Although the combinations of VPD and LAI changes appear to be spatially variable, some regional patterns were still found. For example, 'VPD↑ & LAI↑ & P-ET (-)' is the dominant combination in Mongolian grasslands (Fig. 6a). The increase in LAI due to increased P-ET was also observed in northwest China and northern Central Asia (Fig. 6i, 6k), suggesting that the recent trend of wetting and greening in this region is more likely to be caused by increased surface water availability (Shi et al., 2007). The results of previous coarse regional patterns of dryland change may not necessarily be applicable to the station scale, which needs more station-scale evaluation and validations.

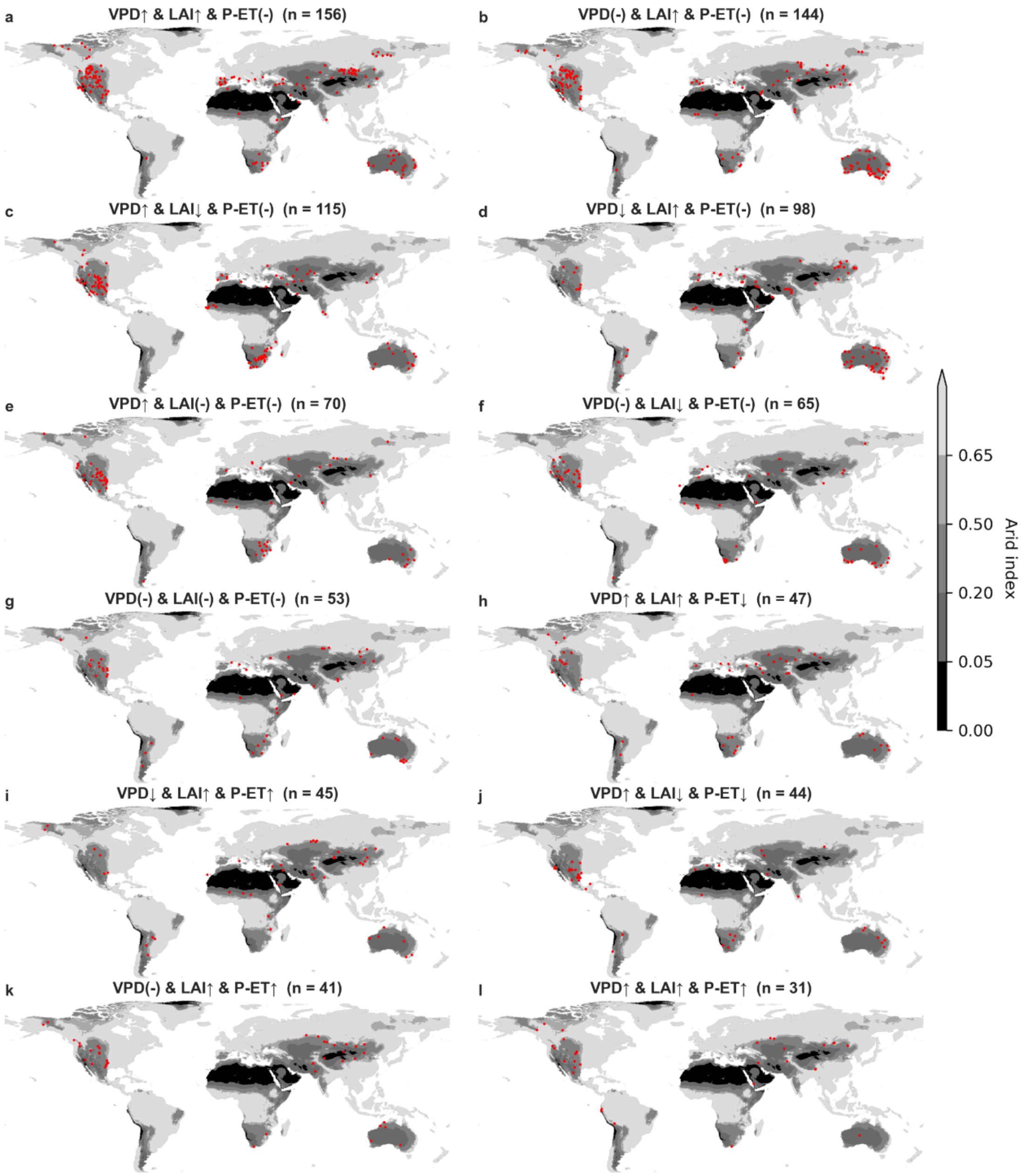

Figure 6 Locations of combinations of VPD, LAI, and P-ET changes from 2003-2010 to 2011-2019. The symbol '↑' represents a significant increase ($p < 0.1$) of VPD, LAI, or P-ET. The symbol '↓' represents a significant decrease ($p < 0.1$) and '(-)' represents insignificant changes.

4. Discussions

4.1 Implications and Perspective

This study investigated the characteristics of dryland change at global dryland meteorological stations using a combination of atmospheric, hydrological, and vegetation indicators. A decoupling between atmospheric, hydrological, and ecological aridity was found in this study, specifically, atmospheric aridity represented by VPD increased, hydrological aridity indicated by P-ET did not change significantly, and ecological aridity represented by LAI decreased. It is consistent with the decoupling found in previous studies based on reanalysis data and coarse-resolution land surface model simulations (Lian et al., 2021) which considered the impacts of elevated CO_2 concentration. This study also found that P-ET showed non-significant changes in most of the dominant combinations of VPD, LAI, and P-ET. This is slightly different from the reported weak aridity hydrological increase in previous studies based on soil moisture and runoff data (Lian et al., 2021), although the year span from 2003 to 2019 in the present study was smaller than these studies (usually more than 50 years).

The value of this study is revisiting the dryland change issue at the station scale. The key to this is the use of a machine learning approach to estimate daily-scale ET data from meteorological stations and to combine the measured P and thus calculate P-ET. Machine learning-based ET simulations (Jung et al., 2010, 2019) may effectively avoid the setting of various hypothetical mechanisms in physics-based ET models ~~(Martens et al., 2017; Zhang et al., 2010; Mu et al., 2011)~~(Martens et al., 2017; Zhang et al., 2010; Mu et al., 2011), mine the relationship between dryland ET and various environmental factors such as climate and vegetation from measured data, and achieve a high estimation accuracy. Therefore, the estimation of P-ET at the station scale effectively measured the status of surface water change since soil moisture and runoff data are difficult to obtain at the meteorological station scale. Station-scale studies of dryland change may be a new direction for the future, given the limitation in the coarse resolution of current reanalysis data, land surface models, etc., and the difficulty of validating their results in the field via ground in situ data. Combined use of climate, hydrological, and vegetation condition variables at the station scale may have the potential to provide an interface for dryland change studies to be more connected to ground observations and associated field experiments. The current satellite remote sensing data still cannot fully capture the physiological and hydraulic characteristics (Zeng et al., 2022) of dryland plants in the context of climate change and extreme weather conditions. It illustrates that station-scale studies will be further important in the future.

4.2 Limitations and Uncertainties

4.2.1 Uncertainties in the ET Estimation

In the past, data for P-ET have rarely been produced at the meteorological station scale, while most in the coarse-resolution grid scale ~~(Jung et al., 2019; Martens et al., 2017; Zhang et al., 2010), and this study combined machine-learning-based estimates of daily ET with actual measurements of P to produce P-ET data for dryland meteorological stations. ET simulations exhibit high accuracy at most stations, but accuracy is limited at a few stations, possibly due to the inefficiency of the selected predictor variables in the explanation of the site-specific ET variations (Shi et al., 2022a). In future studies, it can be effective to incorporate station-specific plant hydraulic characteristics as well as vegetation-trait-related predictor variables (Anderegg, 2015; Anderegg et al., 2018; Shi et al., 2022b; Zhao et al., 2022). In addition, combining data-driven machine learning methods with physical process-based ET estimation models would be promising (Zhao et al., 2019)~~(Jung et al., 2019; Martens et al., 2017; Zhang et al., 2010), and this study combined machine-learning-based estimates of daily ET with actual measurements of P to produce P-ET data for dryland meteorological stations. ET simulations exhibit high accuracy at most stations, but accuracy is limited at a few stations, possibly due to the inefficiency of the selected predictor variables in the explanation of the station-specific ET variations (Shi et al., 2022). In future studies, it can be effective to incorporate station-specific plant hydraulic characteristics as well as vegetation-trait-related predictor variables (Anderegg, 2015; Anderegg et al., 2018; Zhao et al., 2022; Shi et al., 2023). In addition, combining data-driven machine learning methods with physical process-based ET estimation models would be promising (Zhao et al., 2019), with the potential to further improve ET simulation accuracy. In addition, it may be beneficial to combine transpiration observations such as SAPFLUXNET (Poyatos et al., 2021) to provide estimates of transpiration. Compared to ET, transpiration can be more precisely correlated to plant physiological and hydraulic characteristics, thus providing more detailed mechanism interpretations in dryland aridity change.

In addition, mismatches between the flux footprints of flux stations and remote sensing data pixels may also cause uncertainty, especially if the flux footprints include considerable spatial heterogeneity (Chu et al., 2021). The 500 m scale of data extraction in this study may have reduced this effect partially, but it may still exist due to the variability of flux footprints across stations. Previous studies have shown that when data are extracted at scales larger than 500 m, the representativeness of the flux footprint area's land cover types can be considerably decreased (Chu et al., 2021). The use of a fixed target area extent for data extraction may bias model-data integration in multi-station level studies. In the future, to reduce the related bias, we should pay more attention to the heterogeneity within the flux footprints of specific flux stations especially in remote sensing data extraction and processing (Walther et al., 2022).

The low performance of some flux stations (e.g., shrubland stations), may be related to inadequate modelling of the influence of belowground hydrologic processes. Belowground hydrogeologic properties and groundwater dynamics are difficult to quantify directly through remote sensing or meteorological data. It is thus difficult to capture the effects of subterranean ventilation (López-Ballesteros et al., 2017) and the dynamic relationship between plant root zone and groundwater. Previous studies have shown that the root zone storage capacity (Gao et al., 2014; Wang-Erlandsson et al., 2016; Singh et al., 2020) is important in hydrological processes in drylands and during drought events. Researchers have attempted to estimate root depth and root zone storage capacity (Wang-Erlandsson et al., 2016; Stocker et al., 2023), or to couple drylands' deep-root distribution modules into earth system models (Zhang et al., 2013; Li et al., 2015), and improved the hydrological and ecological prediction (Gao et al., 2014). However, in these approaches, there remain partial limitations such as the dependency on satellite-based ET data (Wang-Erlandsson et al., 2016) containing uncertainty. On the other hand, accurately modelling groundwater dynamics remains limited (Gleeson et al., 2016, 2021). Uncertainties in station-scale groundwater dynamics also affect our understanding of the root-groundwater relationship and groundwater's contribution to ET. Combining drought index at different time scales (e.g., the Standardized Precipitation Evapotranspiration Index (SPEI)) at the regional scale (Secci et al., 2021), and the Gravity Recovery and Climate Experiment (GRACE) based anomalies in terrestrial water storage (Li et al., 2019) can be promising in indirectly representing the groundwater dynamics, but mismatches in spatial scales may still cause errors. In addition, our accuracy evaluation was based on the leave-one-station-out cross-validation (Zhang et al., 2021). The validation accuracy may be relatively low when there are no stations with similar environmental conditions in the training set. The RF model that we finally applied to the weather stations included all stations (i.e., no flux station was left), the accuracy can thus be improved a little, especially at weather stations with similar environmental conditions (e.g., shrubland stations) to the previously left flux station in the leave-one-station-out cross-validation.

4.2.2 Spatial and temporal representativeness of meteorological stations on dryland change

Although meteorological stations can provide more accurate climate, hydrology, and vegetation data at fine scales to support studies associated with dryland change, they may still have limitations in spatial and temporal representativeness. First, the temporal representativeness of meteorological stations is highly variable across different regions of the globe. Inconsistencies in the length of station observation records, etc., may lead to unbalance when comparing between regions. Second, meteorological stations are sparsely located in hyperarid areas, and the representativeness of hyperarid regions can be low. In other dryland types (i.e., Dry subhumid, Semiarid, and Arid), the representativeness of meteorological stations may also be affected by other factors such as human activities. In this study, it was considered that irrigation of dryland cropland could greatly affect the assessment of P-ET and VPD, and therefore stations in croplands were removed. However, other disturbances from human activities may still exist, such as possible grazing (Huang et al., 2018) within the 500 m surrounding extent of the station.

In contrast, climate adaptation management in surrounding regions of local meteorological stations may not require much attention to the lack of spatial and temporal representativeness. The combined use of station-scale VPD, LAI, and P-ET data would be valuable for the development of associated adaptation policies in local agriculture management and ecological conservation.

Compared to previous dryland change studies with decades of span, the period in this study is only 2003-2019 due to the constraint of using MODIS-derived data. We split 2003-2019 into two periods with similar year spans, 2003-2010 and 2011-2019. In this way, it is possible to reduce the effect of extreme years when comparing the differences between the two periods. However, the year spans in this study are not very long compared to studies with longer time series (Lian et al., 2021; Huang et al., 2016), and thus the associated findings should be treated with more caution.

5. Conclusion

Combining climatic, hydrological, and vegetation data, this study assesses global dryland change at meteorological ~~sites~~stations from 2003 to 2019. ~~A decoupling between~~It shows that global drylands' atmospheric, hydrological~~,~~ and ecological aridity ~~was found in this study, specifically~~changes are inconsistent. Specifically, atmospheric aridity ~~represented by VPD~~ increased~~, hydrological aridity indicated by machine learning-based P-ET data did not change significantly,~~ and ecological aridity ~~represented by LAI~~ decreased. ~~P-ET showed non-~~Changes in hydrologic aridity were not significant~~-changes~~ in most of the dominant combinations of VPD, LAI, and P-ET. This study highlights the significance to investigate dryland aridity changes using weather station scale data, which can complement previous findings based on coarse-resolution climate reanalysis. It also has the promise of being combined with more station-scale data to provide support for local community's climate change adaptation.

Acknowledgment

We would like to thank Prof. Pierre Gentine for his insightful suggestions on ET modeling.

Financial support

This research was supported by the Tianshan Talent Cultivation (Grant No. 2022TSYCLJ0001), the Key projects of the Natural Science Foundation of Xinjiang Autonomous Region (Grant No. 2022D01D01), the Strategic Priority Research Program of the Chinese Academy of Sciences (Grant No. XDA20060302), and High-End Foreign Experts Project.

Author Contributions

HS and GL initiated this research and were responsible for the integrity of the work as a whole. HS performed formal analysis and calculations and drafted the manuscript. HS was responsible for the data collection and analysis. GL, PDM, TVdV, OH, XH and AK contributed resources and financial support.

Competing interests

The authors declare that they have no conflict of interest.

Code availability

The codes that were used for all analyses are available from the first author (haiyang.shi@hhu.edu.cn).

Data availability

The data used in this study are available from the first author (haiyang.shi@hhu.edu.cn).

References

Anderegg, W. R.: Spatial and temporal variation in plant hydraulic traits and their relevance for climate change impacts on vegetation, New Phytologist, 205, 1008–1014, 2015.

Anderegg, W. R., Konings, A. G., Trugman, A. T., Yu, K., Bowling, D. R., Gabbitas, R., Karp, D. S., Pacala, S., Sperry, J. S., and Sulman, B. N.: Hydraulic diversity of forests regulates ecosystem resilience during drought, Nature, 561, 538–541, 2018.

Berg, A. and McColl, K. A.: No projected global drylands expansion under greenhouse warming, Nat. Clim. Chang., 11, 331–337, https://doi.org/10.1038/s41558-021-01007-8, 2021.

Chu, H., Luo, X., Ouyang, Z., Chan, W. S., Dengel, S., Biraud, S. C., Torn, M. S., Metzger, S., Kumar, J., Arain, M. A., Arkebauer, T. J., Baldocchi, D., Bernacchi, C., Billesbach, D., Black, T. A., Blanken, P. D., Bohrer, G., Bracho, R., Brown, S., Brunsell, N. A., Chen, J., Chen, X., Clark, K., Desai, A. R., Duman, T., Durden, D., Fares, S., Forbrich, I., Gamon, J. A., Gough, C. M., Griffis, T., Helbig, M., Hollinger, D., Humphreys, E., Ikawa, H., Iwata, H., Ju, Y., Knowles, J. F., Knox, S. H., Kobayashi, H., Kolb, T., Law, B., Lee, X., Litvak, M., Liu, H., Munger, J. W., Noormets, A., Novick, K., Oberbauer, S. F., Oechel, W., Oikawa, P., Papuga, S. A., Pendall, E., Prajapati, P., Prueger, J., Quinton, W. L., Richardson, A. D., Russell, E. S., Scott, R. L., Starr, G., Staebler, R., Stoy, P. C., Stuart-Haëntjens, E., Sonnentag, O., Sullivan, R. C., Suyker, A., Ueyama, M., Vargas, R., Wood, J. D., and Zona, D.: Representativeness of Eddy-Covariance flux footprints for areas surrounding AmeriFlux sites, Agricultural and Forest Meteorology, 301–302, 108350, https://doi.org/10.1016/j.agrformet.2021.108350, 2021.

Denissen, J. M., Teuling, A. J., Pitman, A. J., Koirala, S., Migliavacca, M., Li, W., Reichstein, M., Winkler, A. J., Zhan, C., and Orth, R.: Widespread shift from ecosystem energy to water limitation with climate change, Nature Climate Change, 12, 677–684, 2022.

Díaz-Uriarte, R. and Alvarez de Andrés, S.: Gene selection and classification of microarray data using random forest, BMC bioinformatics, 7, 1–13, 2006.

Feng, S. and Fu, Q.: Expansion of global drylands under a warming climate, Atmospheric Chemistry and Physics, 13, 10081–10094, https://doi.org/10.5194/acp-13-10081-2013, 2013.

Feng, S., Gu, X., Luo, S., Liu, R., Gulakhmadov, A., Slater, L. J., Li, J., Zhang, X., and Kong, D.: Greenhouse gas emissions drive global dryland expansion but not spatial patterns of change in aridification, Journal of Climate, 35, 2901–2917, 2022.

Fensholt, R., Langanke, T., Rasmussen, K., Reenberg, A., Prince, S. D., Tucker, C., Scholes, R. J., Le, Q. B., Bondeau, A., and Eastman, R.: Greenness in semi-arid areas across the globe 1981–2007—an Earth Observing Satellite based analysis of trends and drivers, Remote sensing of environment, 121, 144–158, 2012.

Fu, B., Stafford-Smith, M., Wang, Y., Wu, B., Yu, X., Lv, N., Ojima, D. S., Lv, Y., Fu, C., Liu, Y., Niu, S., Zhang, Y., Zeng, H., Liu, Y., Liu, Y., Feng, X., Zhang, L., Wei, Y., Xu, Z., Li, F., Cui, X., Diop, S., and Chen, X.: The Global-DEP conceptual framework — research on dryland ecosystems to promote sustainability, Current Opinion in Environmental Sustainability, 48, 17–28, https://doi.org/10.1016/j.cosust.2020.08.009, 2021.

Gao, H., Hrachowitz, M., Schymanski, S., Fenicia, F., Sriwongsitanon, N., and Savenije, H.: Climate controls how ecosystems size the root zone storage capacity at catchment scale, Geophysical Research Letters, 41, 7916–7923, 2014.

Gleeson, T., Befus, K. M., Jasechko, S., Luijendijk, E., and Cardenas, M. B.: The global volume and distribution of modern groundwater, Nature Geoscience, 9, 161–167, 2016.

Gleeson, T., Wagener, T., Döll, P., Zipper, S. C., West, C., Wada, Y., Taylor, R., Scanlon, B., Rosolem, R., and Rahman, S.: GMD Perspective: The quest to improve the evaluation of groundwater representation in continental to global scale models, Geoscientific Model Development Discussions, 2021, 1–59, 2021.

Grömping, U.: Variable importance assessment in regression: linear regression versus random forest, The American Statistician, 63, 308–319, 2009.

Grünzweig, J. M., De Boeck, H. J., Rey, A., Santos, M. J., Adam, O., Bahn, M., Belnap, J., Deckmyn, G., Dekker, S. C., Flores, O., Gliksman, D., Helman, D., Hultine, K. R., Liu, L., Meron, E., Michael, Y., Sheffer, E., Throop, H. L., Tzuk, O., and Yakir, D.: Dryland mechanisms could widely control ecosystem functioning in a drier and warmer world, Nat Ecol Evol, 6, 1064–1076, https://doi.org/10.1038/s41559-022-01779-y, 2022.

He, B., Wang, S., Guo, L., and Wu, X.: Aridity change and its correlation with greening over drylands, Agricultural and Forest Meteorology, 278, 107663, https://doi.org/10.1016/j.agrformet.2019.107663, 2019.

Hickler, T., Eklundh, L., Seaquist, J. W., Smith, B., Ardö, J., Olsson, L., Sykes, M. T., and Sjöström, M.: Precipitation controls Sahel greening trend, Geophysical Research Letters, 32, 2005.

Howell, T. A. and Dusek, D. A.: Comparison of vapor-pressure-deficit calculation methods--Southern High Plains, 1995.

Huang, J., Yu, H., Guan, X., Wang, G., and Guo, R.: Accelerated dryland expansion under climate change, Nature Clim Change, 6, 166–171, https://doi.org/10.1038/nclimate2837, 2016.

Huang, J., Li, Y., Fu, C., Chen, F., Fu, Q., Dai, A., Shinoda, M., Ma, Z., Guo, W., Li, Z., Zhang, L., Liu, Y., Yu, H., He, Y., Xie, Y., Guan, X., Ji, M., Lin, L., Wang, S., Yan, H., and Wang, G.: Dryland climate change: Recent progress and challenges, Reviews of Geophysics, 55, 719–778, https://doi.org/10.1002/2016RG000550, 2017.

Huang, X., Luo, G., Ye, F., and Han, Q.: Effects of grazing on net primary productivity, evapotranspiration and water use efficiency in the grasslands of Xinjiang, China, Journal of Arid Land, 10, 588–600, 2018.

Jung, M., Reichstein, M., Ciais, P., Seneviratne, S. I., Sheffield, J., Goulden, M. L., Bonan, G., Cescatti, A., Chen, J., de Jeu, R., Dolman, A. J., Eugster, W., Gerten, D., Gianelle, D., Gobron, N., Heinke, J., Kimball, J., Law, B. E., Montagnani, L., Mu, Q., Mueller, B., Oleson, K., Papale, D., Richardson, A. D., Roupsard, O., Running, S., Tomelleri, E., Viovy, N., Weber, U., Williams, C., Wood, E., Zaehle, S., and Zhang, K.: Recent decline in the global land evapotranspiration trend due to limited moisture supply, Nature, 467, 951–954, https://doi.org/10.1038/nature09396, 2010.

Jung, M., Koirala, S., Weber, U., Ichii, K., Gans, F., Camps-Valls, G., Papale, D., Schwalm, C., Tramontana, G., and Reichstein, M.: The FLUXCOM ensemble of global land-atmosphere energy fluxes, Sci Data, 6, 74, https://doi.org/10.1038/s41597-019-0076-8, 2019.

Li, B., Rodell, M., Kumar, S., Beaudoing, H. K., Getirana, A., Zaitchik, B. F., de Goncalves, L. G., Cossetin, C., Bhanja, S., and Mukherjee, A.: Global GRACE data assimilation for groundwater and drought monitoring: Advances and challenges, Water Resources Research, 55, 7564–7586, 2019.

Li, C., Zhang, C., Luo, G., Chen, X., Maisupova, B., Madaminov, A. A., Han, Q., and Djenbaev, B. M.: Carbon stock and its responses to climate change in C entral A sia, Global change biology, 21, 1951–1967, 2015.

Li, C., Fu, B., Wang, S., Stringer, L. C., Wang, Y., Li, Z., Liu, Y., and Zhou, W.: Drivers and impacts of changes in China's drylands, Nat Rev Earth Environ, 2, 858–873, https://doi.org/10.1038/s43017-021-00226-z, 2021.

Lian, X., Piao, S., Chen, A., Huntingford, C., Fu, B., Li, L. Z. X., Huang, J., Sheffield, J., Berg, A. M., Keenan, T. F., McVicar, T. R., Wada, Y., Wang, X., Wang, T., Yang, Y., and Roderick, M. L.: Multifaceted characteristics of dryland aridity changes in a warming world, Nat Rev Earth Environ, 2, 232–250, https://doi.org/10.1038/s43017-021-00144-0, 2021.

López-Ballesteros, A., Serrano-Ortiz, P., Kowalski, A. S., Sánchez-Cañete, E. P., Scott, R. L., and Domingo, F.: Subterranean ventilation of allochthonous CO2 governs net CO2 exchange in a semiarid Mediterranean grassland, Agricultural and Forest Meteorology, 234–235, 115–126, https://doi.org/10.1016/j.agrformet.2016.12.021, 2017.

Martens, B., Miralles, D. G., Lievens, H., Van Der Schalie, R., De Jeu, R. A., Fernández-Prieto, D., Beck, H. E., Dorigo, W. A., and Verhoest, N. E.: GLEAM v3: Satellite-based land evaporation and root-zone soil moisture, Geoscientific Model Development, 10, 1903–1925, 2017.

Milly, P. C. D. and Dunne, K. A.: Potential evapotranspiration and continental drying, Nature Clim Change, 6, 946–949, https://doi.org/10.1038/nclimate3046, 2016.

Mu, Q., Zhao, M., and Running, S. W.: Improvements to a MODIS global terrestrial evapotranspiration algorithm, Remote Sensing of Environment, 115, 1781–1800, https://doi.org/10.1016/j.rse.2011.02.019, 2011.

Pan, N., Wang, S., Liu, Y., Li, Y., Xue, F., Wei, F., Yu, H., and Fu, B.: Rapid increase of potential evapotranspiration weakens the effect of precipitation on aridity in global drylands, Journal of Arid Environments, 186, 104414, https://doi.org/10.1016/j.jaridenv.2020.104414, 2021.

Poulter, B., Frank, D., Ciais, P., Myneni, R. B., Andela, N., Bi, J., Broquet, G., Canadell, J. G., Chevallier, F., and Liu, Y. Y.: Contribution of semi-arid ecosystems to interannual variability of the global carbon cycle, Nature, 509, 600–603, 2014.

Poyatos, R., Granda, V., Flo, V., Adams, M. A., Adorján, B., Aguadé, D., Aidar, M. P., Allen, S., Alvarado-Barrientos, M. S., and Anderson-Teixeira, K. J.: Global transpiration data from sap flow measurements: the SAPFLUXNET database, Earth System Science Data, 13, 2607–2649, 2021.

Prăvălie, R.: Drylands extent and environmental issues. A global approach, Earth-Science Reviews, 161, 259–278, https://doi.org/10.1016/j.earscirev.2016.08.003, 2016.

Programme, U. N. E.: World Atlas of Desertification: Second Edition, 1997.

Ramón Vallejo, V., Smanis, A., Chirino, E., Fuentes, D., Valdecantos, A., and Vilagrosa, A.: Perspectives in dryland restoration: approaches for climate change adaptation, New Forests, 43, 561–579, 2012.

Reynolds, J. F., Smith, D. M. S., Lambin, E. F., Turner, B. L., Mortimore, M., Batterbury, S. P. J., Downing, T. E., Dowlatabadi, H., Fernández, R. J., Herrick, J. E., Huber-Sannwald, E., Jiang, H., Leemans, R., Lynam, T., Maestre, F. T., Ayarza, M., and Walker, B.: Global Desertification: Building a Science for Dryland Development, Science, 316, 847–851, https://doi.org/10.1126/science.1131634, 2007.

Roderick, M. L., Greve, P., and Farquhar, G. D.: On the assessment of aridity with changes in atmospheric CO 2, Water Resources Research, 51, 5450–5463, 2015.

Ryu, Y., Jiang, C., Kobayashi, H., and Detto, M.: MODIS-derived global land products of shortwave radiation and diffuse and total photosynthetically active radiation at 5 km resolution from 2000, Remote Sensing of Environment, 204, 812–825, https://doi.org/10.1016/j.rse.2017.09.021, 2018.

Secci, D., Tanda, M. G., D'Oria, M., Todaro, V., and Fagandini, C.: Impacts of climate change on groundwater droughts by means of standardized indices and regional climate models, Journal of Hydrology, 603, 127154, https://doi.org/10.1016/j.jhydrol.2021.127154, 2021.

Shi, H., Luo, G., Hellwich, O., Xie, M., Zhang, C., Zhang, Y., Wang, Y., Yuan, X., Ma, X., Zhang, W., Kurban, A., De Maeyer, P., and Van de Voorde, T.: Evaluation of water flux predictive models developed using eddy-covariance observations and machine learning: a meta-analysis, Hydrology and Earth System Sciences, 26, 4603–4618, https://doi.org/10.5194/hess-26-4603-2022, ~~2022a~~2022.

Shi, H., Luo, G., Hellwich, O., Kurban, A., De Maeyer, P., and Van de Voorde, T.: Revisiting and attributing the global controls ~~on~~over terrestrial ecosystem functions of climate and plant traits at FLUXNET sites ~~with~~via causal ~~networks~~graphical models, Biogeosciences ~~Discussions, 1–22~~, 20, 2727–2741, https://doi.org/10.5194/bg-~~2022-191, 2022b~~20-2727-2023, 2023.

Shi, Y., Shen, Y., Kang, E., Li, D., Ding, Y., Zhang, G., and Hu, R.: Recent and future climate change in northwest China, Climatic change, 80, 379–393, 2007.

Singh, C., Wang-Erlandsson, L., Fetzer, I., Rockström, J., and Van Der Ent, R.: Rootzone storage capacity reveals drought coping strategies along rainforest-savanna transitions, Environmental Research Letters, 15, 124021, 2020.

Stocker, B. D., Tumber-Dávila, S. J., Konings, A. G., Anderson, M. C., Hain, C., and Jackson, R. B.: Global patterns of water storage in the rooting zones of vegetation, Nat. Geosci., 16, 250–256, https://doi.org/10.1038/s41561-023-01125-2, 2023.

Strobl, C., Boulesteix, A.-L., Kneib, T., Augustin, T., and Zeileis, A.: Conditional variable importance for random forests, BMC Bioinformatics, 9, 307, https://doi.org/10.1186/1471-2105-9-307, 2008.

Tramontana, G., Jung, M., Schwalm, C. R., Ichii, K., Camps-Valls, G., Ráduly, B., Reichstein, M., Arain, M. A., Cescatti, A., Kiely, G., Merbold, L., Serrano-Ortiz, P., Sickert, S., Wolf, S., and Papale, D.: Predicting carbon dioxide and energy fluxes across global FLUXNET sites with regression algorithms, Biogeosciences, 13, 4291–4313, https://doi.org/10.5194/bg-13-4291-2016, 2016.

Walther, S., Besnard, S., Nelson, J. A., El-Madany, T. S., Migliavacca, M., Weber, U., Carvalhais, N., Ermida, S. L., Brümmer, C., Schrader, F., Prokushkin, A. S., Panov, A. V., and Jung, M.: Technical note: A view from space on global flux towers by MODIS and Landsat: the FluxnetEO data set, Biogeosciences, 19, 2805–2840, https://doi.org/10.5194/bg-19-2805-2022, 2022.

Wang-Erlandsson, L., Bastiaanssen, W. G., Gao, H., Jägermeyr, J., Senay, G. B., Van Dijk, A. I., Guerschman, J. P., Keys, P. W., Gordon, L. J., and Savenije, H. H.: Global root zone storage capacity from satellite-based evaporation, Hydrology and Earth System Sciences, 20, 1459–1481, 2016.

Yang, Y., Zhang, S., McVicar, T. R., Beck, H. E., Zhang, Y., and Liu, B.: Disconnection Between Trends of Atmospheric Drying and Continental Runoff, Water Resources Research, 54, 4700–4713, https://doi.org/10.1029/2018WR022593, 2018.

Yao, J., Liu, H., Huang, J., Gao, Z., Wang, G., Li, D., Yu, H., and Chen, X.: Accelerated dryland expansion regulates future variability in dryland gross primary production, Nat Commun, 11, 1665, https://doi.org/10.1038/s41467-020-15515-2, 2020.

Yao, Y., Liu, Y., Wang, Y., and Fu, B.: Greater increases in China's dryland ecosystem vulnerability in drier conditions than in wetter conditions, Journal of Environmental Management, 291, 112689, 2021.

Zeng, Y., Hao, D., Huete, A., Dechant, B., Berry, J., Chen, J. M., Joiner, J., Frankenberg, C., Bond-

Lamberty, B., Ryu, Y., Xiao, J., Asrar, G. R., and Chen, M.: Optical vegetation indices for monitoring terrestrial ecosystems globally, Nat Rev Earth Environ, 1–17, https://doi.org/10.1038/s43017-022-00298-5, 2022.

Zhang, C., Li, C., Luo, G., and Chen, X.: Modeling plant structure and its impacts on carbon and water cycles of the Central Asian arid ecosystem in the context of climate change, Ecological Modelling, 267, 158–179, https://doi.org/10.1016/j.ecolmodel.2013.06.008, 2013.

Zhang, C., Luo, G., Hellwich, O., Chen, C., Zhang, W., Xie, M., He, H., Shi, H., and Wang, Y.: A framework for estimating actual evapotranspiration at weather stations without flux observations by combining data from MODIS and flux towers through a machine learning approach, Journal of Hydrology, 603, 127047, https://doi.org/10.1016/j.jhydrol.2021.127047, 2021.

Zhang, K., Kimball, J. S., Nemani, R. R., and Running, S. W.: A continuous satellite-derived global record of land surface evapotranspiration from 1983 to 2006, Water ~~Resources Research,~~Resour. Res., 46, https://doi.org/10.1029/2009WR008800, 2010.

Zhao, M., A, G., Liu, Y., and Konings, A. G.: Evapotranspiration frequently increases during droughts, Nat. Clim. Chang., 12, 1024–1030, https://doi.org/10.1038/s41558-022-01505-3, 2022.

Zhao, W. L., Gentine, P., Reichstein, M., Zhang, Y., Zhou, S., Wen, Y., Lin, C., Li, X., and Qiu, G. Y.: Physics-Constrained Machine Learning of Evapotranspiration, Geophysical Research Letters, 46, 14496–14507, https://doi.org/10.1029/2019GL085291, 2019.

Zhu, Z., Piao, S., Myneni, R. B., Huang, M., Zeng, Z., Canadell, J. G., Ciais, P., Sitch, S., Friedlingstein, P., and Arneth, A.: Greening of the Earth and its drivers, Nature climate change, 6, 791–795, 2016.